

Geodesic Paths Approach to Color Image Enhancement

M. Szczepanski¹, B. Smolka, and D. Slusarczyk

*Department of Automatic Control
Silesian University of Technology
Akademicka 16 Str, 44-101 Gliwice, Poland*

K. N. Plataniotis² and A. N. Venetsanopoulos

*Edward S. Rogers Sr. Department of Electrical and Computer Engineering
University of Toronto
10 King's College Road, Toronto, Canada*

Abstract

New filter class for multichannel image processing is introduced and analyzed. The new technique of image enhancement is capable of reducing impulsive and Gaussian noise and it significantly outperforms the standard methods of noise reduction. In the paper a smoothing operator, based on a random walk model and a fuzzy similarity measure between pixels connected by a digital geodesic path is introduced. The efficiency of the proposed method was tested on the standard color images using the objective image quality measures. Obtained results show that the new method not only outperforms standard noise reduction algorithms, but has some interesting features useful for segmentation of noisy color images.

1 Introduction

Numerous noise filtering techniques have been proposed for multichannel image processing [6,7]. The nonlinear filters are required to preserve edges, corners and other image details, and to remove Gaussian and impulsive noise. One of the most important families of nonlinear filters is based on order statistics. A number of different vector processing filters using order statistics have been developed in the last decade. The output of these filters is defined as the lowest ranked vector according to a specific vector ordering technique.

¹ Email: mszczepa@ia.polsl.gliwice.pl

² Email: kostas@dsp.toronto.edu

Let $\mathbf{F}(x)$ represents a multichannel image and let W be a window of finite size n (filter length). The noisy image vectors inside the filtering window W are denoted as \mathbf{F}_j , $j = 0, 1, \dots, n - 1$. If the distance between two vectors $\mathbf{F}_i, \mathbf{F}_j$ is denoted as $\rho(\mathbf{F}_i, \mathbf{F}_j)$ then the scalar quantity $R_i = \sum_{j=0}^{n-1} \rho(\mathbf{F}_i, \mathbf{F}_j)$, is the distance associated with the noisy vector \mathbf{F}_i . The ordering of the R_i 's: $R_{(0)} \leq R_{(1)} \leq \dots \leq R_{(n-1)}$, implies the same ordering to the corresponding vectors $\mathbf{F}_i : \mathbf{F}_{(0)} \leq \mathbf{F}_{(1)} \leq \dots \leq \mathbf{F}_{(n-1)}$. Nonlinear ranked type multichannel estimators define the vector $\mathbf{F}_{(0)}$ as the filter output.

The best known order statistics filter is the so called Vector Median Filter (VMF). The definition of the multichannel median is a direct extension of the ordinary single-channel median definition [1]. VMF uses the L_1 or L_2 norm to order vectors according to their relative magnitude differences.

The orientation difference between color vectors can also be used to remove vectors with atypical directions (*Vector Directional Filter* - VDF, *Basic Vector Directional Filter* - BVDF) [14]

Another efficient rank-ordered technique called Hybrid Directional Filter was presented in [4]. This filter operates on the directional and the magnitude of the color vectors independently and then combines them to produce a unique final output. Another more complex hybrid filter, which involves the utilization of an Arithmetic Mean Filter (AMF), has also been proposed [4].

The reduction of image noise without major degradation of the image structure is one of the most important problems of the low-level image processing. A whole variety of algorithms has been developed, however none of them can be seen as a final solution of the noise problem and therefore a new filtering technique is proposed in this paper.

2 Digital Paths Approach

Let us assume, that \mathbb{R}^2 is the Euclidean space, W is a planar subset of \mathbb{R}^2 and x, y are points of the set W . A path from x to y is a continuous mapping $\mathcal{P}: [a, b] \rightarrow X$, such that $\mathcal{P}(a) = x$ and $\mathcal{P}(b) = y$. Point x is the starting point and y is the ending point of the path \mathcal{P} [2].

An increasing polygonal line P on the path \mathcal{P} is any polygonal line $P = \{g(\lambda_i)\}_{i=0}^n$, $a = \lambda_0 < \dots < \lambda_n = b$. The length of the polygonal line P is the total sum of its constitutive line segments $L(P) = \sum_{i=1}^n \rho(\mathcal{P}(\lambda_{i-1}), \mathcal{P}(\lambda_i))$ where $\rho(x, y)$ is the distance between the points x and y , when a specific metric is adopted. If \mathcal{P} is a path from x to y then it is called rectifiable, if and only if $L(P)$, where P is an increasing polygonal line, is bounded. Its upper bound is called the length of the path \mathcal{P} .

The geodesic distance $\rho^W(x, y)$ between points x and y is the lower bound of the length of all paths leading from x to y totally included in W . If such paths do not exist, then the value of the geodesic distance is set to ∞ . The geodesic distance verifies $\rho^W(x, y) \geq \rho(x, y)$ and in the case when W is a convex set then $\rho^W(x, y) = \rho(x, y)$.

The notion of the path can be extended to a lattice, which is a set of discrete points, in our case image pixels. Let a digital lattice $\mathcal{H} = (\mathbf{F}, \mathcal{N})$ be defined by \mathbf{F} , which is the set of all points of the plane (pixels of a color image) and the neighborhood relation \mathcal{N} between the lattice points [11].

A digital path $P = \{p_i\}_{i=0}^n$ on the lattice \mathcal{H} is a sequence of neighboring points $(p_{i-1}, p_i) \in \mathcal{N}$. The length $L(P)$ of digital path $P \{p_i\}_{i=0}^n$ is simply $\sum_{i=1}^n \rho^{\mathcal{H}}(p_{i-1}, p_i)$, where $\rho^{\mathcal{H}}$ denotes the distance between two neighboring points on the lattice \mathcal{H} (Fig. 1).

Constraining the paths to be totally included in a predefined set $W \in \mathbf{F}$ yields the digital geodesic distance ρ^W . In this paper we will assign to the distance of neighboring points the value 1 and will be working with the 8-neighborhood system.

Let the pixels (i, j) and (k, l) be called connected (denoted as $(i, j) \leftrightarrow (k, l)$), if there exists a geodesic path $P^W \{(i, j), (k, l)\}$ contained in the set W starting from (i, j) and ending at (k, l) .

If two pixels (x_0, y_0) and (x_n, y_n) are connected by a geodesic path $P_m^W \{(x_0, y_0), (x_1, y_1), \dots, (x_n, y_n)\}$ of length n then let $\chi_m^{W,n}$

$$\chi_m^{W,n} \{(x_0, y_0), (x_n, y_n)\} = \sum_{k=0}^{n-1} \|\mathbf{F}(x_{k+1}, y_{k+1}) - \mathbf{F}(x_k, y_k)\|, \quad (1)$$

where m is the path index be a measure of dissimilarity between pixels (x_0, y_0) and (x_n, y_n) , along a specific geodesic path P_m^W joining (x_0, y_0) and (x_n, y_n) [13,3]. If a path joining two distinct points x, y , such that $\mathbf{F}(x) = \mathbf{F}(y)$ consists of lattice points of the same values, then $\chi^{W,n}(x, y) = 0$ otherwise $\chi^{W,n}(x, y) > 0$.

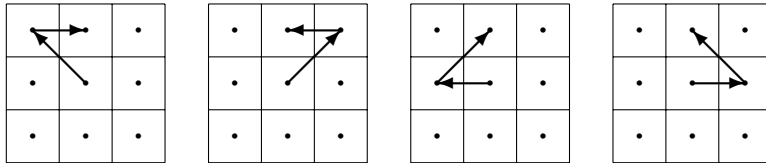


Fig. 1. There are four geodesic paths of length 2 connecting two neighboring points contained in the specific window W when the 8-neighborhood system is applied.

Let us now define a fuzzy similarity function between two pixels connected along all geodesic digital paths leading from (i, j) to (k, l)

$$\mu^{W,n} \{(i, j), (k, l)\} = \frac{1}{\omega} \sum_{m=1}^{\omega} \exp [-\beta \cdot \chi_m^{W,n} \{(i, j), (k, l)\}] \quad (2)$$

where ω is the number of all paths connecting (i, j) and (k, l) , β is a design parameter and $\chi_m^{W,n} \{(i, j), (k, l)\}$ is a dissimilarity value along a specific path from a set of all ω possible paths leading from (i, j) to (k, l) . In this way $\mu^{W,n} \{(i, j), (k, l)\}$ is a value, taken over all routes linking the starting point

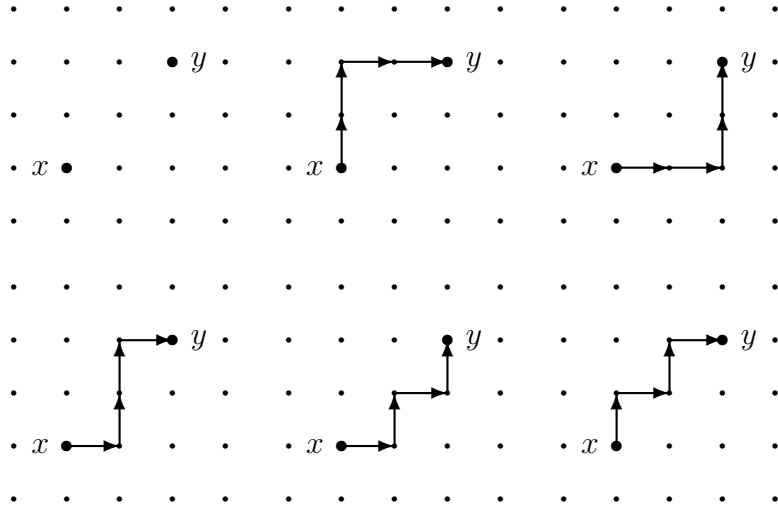


Fig. 2. There are five paths of length 4 connecting point x and y when the 4-neighborhood system is used.

(i, j) and the endpoint (k, l) . For $n = 1$ and W a square mask of the size 3×3 (Fig. 1), we have

$$\mu^{W,1}\{(i, j), (k, l)\} = \exp\{-\beta||\mathbf{F}(i, j) - \mathbf{F}(k, l)||\}, \quad (3)$$

and when $\mathbf{F}(i, j) = \mathbf{F}(k, l)$ then $\chi^{W,n}\{(i, j), (k, l)\} = 0$, $\mu\{(i, j), (k, l)\} = 1$, and for $||\mathbf{F}(i, j) - \mathbf{F}(k, l)|| \rightarrow \infty$ then $\mu \rightarrow 0$ [8]. The normalized similarity function takes the form

$$\psi^{W,n}\{(i, j), (k, l)\} = \frac{\mu^{W,n}\{(i, j), (k, l)\}}{\sum_{(l, m) \leftrightarrow (i, j)} \mu^{W,n}\{(i, j), (l, m)\}}. \quad (4)$$

and has the property that

$$\sum_{(k, l) \leftrightarrow (i, j)} \psi^{W,n}\{(i, j), (k, l)\} = 1. \quad (5)$$

Now we are in a position to define a smoothing transformation $\hat{\mathbf{F}}$

$$\hat{\mathbf{F}}(i, j) = \sum_{(k, l) \leftrightarrow (i, j)} \psi^{W,n}\{(i, j), (k, l)\} \cdot \mathbf{F}(k, l), \quad (6)$$

where (k, l) are points which are connected with (i, j) by geodesic digital paths of length n included in W .

3 New Filter Design

3.1 Models of Digital Paths

The features of the new filter strongly depend on the type of digital paths chosen. Numerous models of paths produce specific filters with the ability to suppress certain kinds of noise. In this paper three types of random paths are introduced: Self avoiding path (*SAP*) Non-reversing path model (*NRP*) and Escaping Path Model (*EPM*)(Fig. 3).

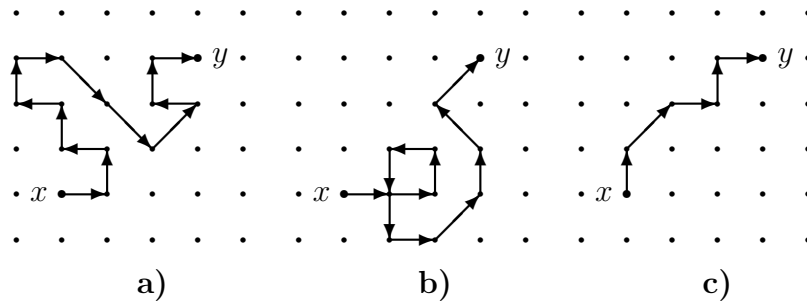


Fig. 3. Different types of geodesic paths **a)** Self avoiding path (*SAP*), **b)** Non-reversing path (*NRP*), **c)** Escaping Path (*EPM*) with L_2 metric .

Self avoiding path (*SAP*) is a special path along the image lattice such that adjacent pairs of edges in the sequence share a common vertex of the lattice, but no vertex is visited more than once and in this way the trajectory never intersects itself. In other words *SAP* is a path on a lattice that does not pass through the same point twice (Fig. 3a).

On the two-dimensional lattice *SAP* is a finite sequence of distinct lattice points $(x_0, y_0), (x_1, y_1), \dots, (x_n, y_n)$, which are in neighborhood relation and $(x_i, y_i) \neq (x_j, y_j)$ for all $i \neq j$.

Non-reversing path is (*NRP*) is a special trajectory along the image lattice such that adjacent pairs of edges in the sequence share a common vertex of the lattice, but no vertex can be revisited in one step (Fig. 3b).

Escaping path model(*EPM*) is a model of random walk in which the distance from the starting point cannot be decreased in subsequent steps (Fig. 3c).

For two steps all described paths are equivalent.

3.2 Iterative Nature of the New Class of Filters

The smoothing operator $\hat{\mathbf{F}}$ in (6) has to be applied in an iterative way. Starting with low value of β enables the smoothing of the image noise components. At each iteration steps the parameter β has to be increased, like in simulated

annealing, so we have used:

$$\beta(k) = \beta(k-1) \cdot \alpha, \quad k = 1, \dots, n, \quad (7)$$

However, in this case two parameters α and β are needed to define the filter. In order to make the new filter less dependent on the initial parameter values, adaptive version of our filter was introduced. Parameter β in (2) is obtained from the data in the filter window and is defined as a standard deviation of samples in W , multiplied by a normalizing constant factor γ ,

$$\beta = \frac{\gamma}{N \cdot l} \sqrt{\sum_{i,j \in W} \sum_{k=1}^l (F_k(i,j) - \bar{F}_k)^2}, \quad (8)$$

where N is the number of pixels in the processing window W , l is the number of channels of the image (in the RGB color space $l = 3$), \bar{F}_k denotes the average value of the k th component in window W and γ is a normalizing parameter. Using adaptive version of our filter, there is no need to use parameter α from (7) and in this way there remains only one design parameter, while performing the filtering. As shown in Tabs. 2 and 3 the adaptive version of our filter yields better results especially for heavily distorted images.

4 Results

The effectiveness of the new filters was tested on the color test image *LENA* contaminated by a Gaussian noise of $\sigma = 30$ and on the same original image contaminated by 4% impulsive noise (salt & pepper in each channel) mixed with Gaussian noise ($\sigma = 30$). The performance of the presented method was evaluated by means of the objective image quality measures RMSE, PSNR, NMSE and NCD [7].

Tables 2 and 3 show the results obtained for $n = 2$ and $n = 3$ in comparison with the standard noise reduction algorithms shown in Tab. 1. Additionally Fig. 7 shows the comparison of the new filtering technique with the standard vector median.

In our experiments wide range of filter parameters was examined. Figures 4 and 5 show the peak signal to noise ratio (PSNR) and normalized color distance (NCD) dependence on the α and β values for the *LENA* standard image corrupted by 4% impulse mixed with Gaussian noise ($\sigma = 30$). As can be easily observed the extrema of PSNR and NCD are rather flat and in this way the new filter is robust to improper values of chosen parameters. Results obtained for adaptive version of our filter are presented in Fig. 6

For the calculation of the similarity function we used the L_1 metric and an exponential function, however we have obtained good results using other convex functions and different vector metrics.

Notation	METHOD	REF.
AMF	Arithmetic Mean Filter	[7]
VMF	Vector Median Filter	[1]
BVDF	Basic Vector Directional Filter	[14]
GVDF	Generalized Vector Directional Filter	[15]
DDF	Directional-Distance Filter	[5]
HDF	Hybrid Directional Filter	[4]
AHDF	Adaptive Hybrid Directional Filter	[4]
FVDF	Fuzzy Vector Directional Filter	[8]
ANNF	Adaptive Nearest Neighbor Filter	[9]
ANP-EF	Adaptive Non Parametric (Exponential) Filter	[10]
ANP-GF	Adaptive Non Parametric (Gaussian) Filter	[10]
ANP-DF	Adaptive Non Parametric (Directional) Filter	[10]
VBAMMF	Vector Bayesian Adaptive Median/Mean Filter	[10]

Table 1

Filters taken for comparison with the proposed noise reduction technique.

The efficiency of the new algorithm as compared with the vector median filter is shown in Figs. 7 and 8. After the application of the new filter, the impulse pixels introduced by noise process are removed, the contrast is improved, the image is smoothed and what is important the edges are well preserved.

Figures 9 and 10 show the features of the new filter class for *LENA* and *PEPPERS* images. The results show that they are quite similar to those obtained using anisotropic diffusion. However, our filter is robust to the impulse noise, which is a main obstacle, when using the anisotropic diffusion approach to smooth noisy images.

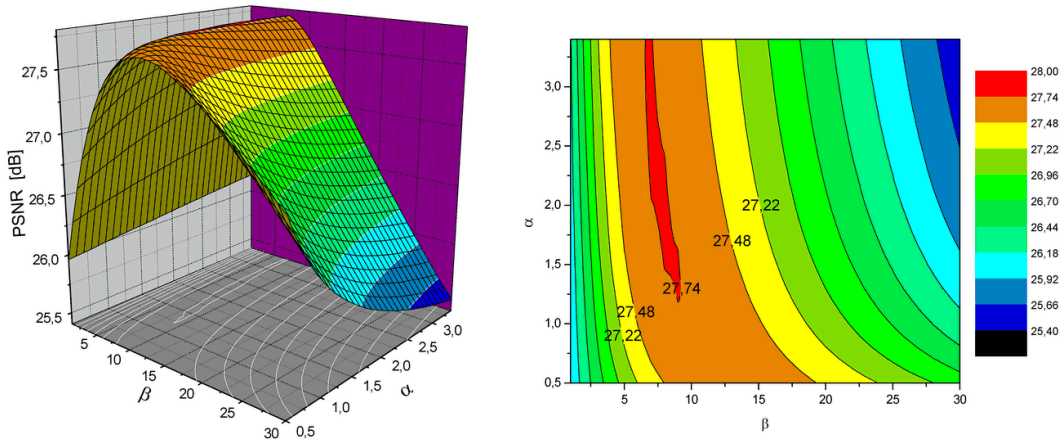


Fig. 4. Efficiency of the new filter in terms of PSNR and its dependence on the α and β values for the *LENA* standard image corrupted by 4% impulse and Gaussian noise ($\sigma = 30$) (SAP $n = 3$, 2 iterations).

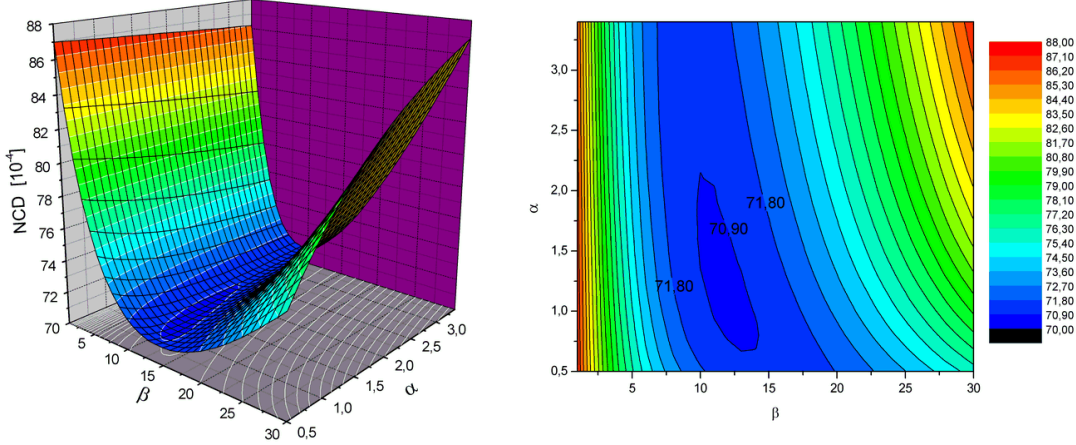


Fig. 5. Efficiency of the new filter in terms of NCD and its dependence on the α and β values for *LENA* standard image corrupted by 4% impulse and Gaussian noise ($\sigma = 30$) (SAP $n = 3$, 2 iterations).

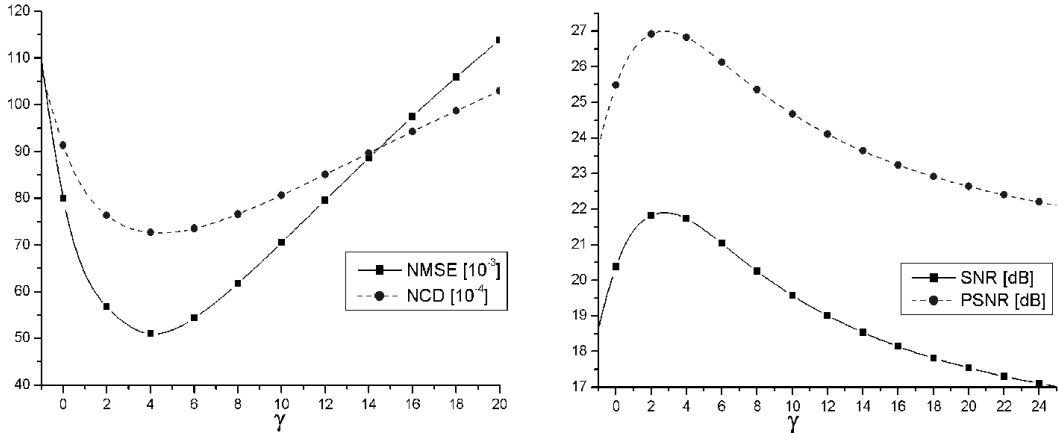


Fig. 6. Efficiency of the new adaptive filter in terms of PSNR, SNR, NCD and NMSE for *LENA* standard image corrupted by 4% impulse and Gaussian noise ($\sigma = 30$) ($n = 2$, 2 iterations).

5 Conclusions

In this paper, a new class of filters for noise reduction in color images has been presented. Experimental results indicate that the new filtering technique outperforms the standard procedures used to reduce mixed impulsive and Gaussian noise in color images. The new methods have some interesting features useful for segmentation of noisy color images. Especially, filters based on the escaping path models (*EPP*), have the ability of segmentation of strongly disturbed images (Fig. 8). The efficiency of the new filtering techniques are shown in Tabs. 2 and 3 and in Figs. 7, 8.



Fig. 7. Comparison of efficiency of the vector median with the new filter proposed in this paper **a)** test image (part of a scanned map), **b)** result of the standard vector median filtration (3×3 mask), **c)** result of the filtration with the new filter using SAP ($\beta = 20, \alpha = 1.25, n = 2, 3$ iterations)

References

- [1] Astola J., Haavisto P., Neuovo Y., *Vector median filters*, IEEE Proc., **78** (1990), 678-689
- [2] Borgefors G., *Distances transformations in digital images*, Computer Vision, Graphics and Image Processing, **34** (1986) 334-371
- [3] Cuisenaire O., "Distance transformations: fast algorithms and applications to medical image processing", PhD Thesis, Universite Catholique de Louvain, Oct. 1999

- [4] Gabbouj M., Cheickh F.A., *Vector median - vector directional hybrid filter for colour image restoration*, Proceedings of EUSIPCO, 879-881, 1996
- [5] Karakos D., Trahanias P.E., *Generalized multichannel image filtering structures*, IEEE Trans. on Image Processing, 6, (7), 1038-1045, 1997
- [6] Pitas I., Venetsanopoulos A. N, "Nonlinear Digital Filters : Principles and Applications", Kluwer Academic Publishers, Boston, MA, 1990
- [7] Plataniotis K.N., Venetsanopoulos A.N., "Color Image Processing and Applications", Springer Verlag, (June 2000)
- [8] Plataniotis K.N., Androutsos D., Venetsanopoulos A.N.V., *Fuzzy adaptive filters for multichannel image processing*, Signal Processing Journal, 55, (1), 93-106, 1996
- [9] Plataniotis K.N., Androutsos D., Sri V., Venetsanopoulos A.N.V., *A nearest neighbor multichannel filter*, Electronic Letters, 1910-1911, 1995
- [10] Plataniotis K.N., Androutsos D., Vinayagamoorthy S., Venetsanopoulos A.N.V., *Color image processing using adaptive multichannel filters*, IEEE Trans. on Image Processing, 6 (7), 933-950, 1997
- [11] Schmitt M., *Lecture Notes on Geodesy and Morphological Measurements*, Proceedings of the Summer School on Morphological Image and Signal Processing, Zakopane, Poland (1995)
- [12] Smolka B., Wojciechowski K., *Random walk approach to image enhancement*, Signal Processing, Vol. 81, No. 3, 465-482, 2001
- [13] Toivanen P.J., *New geodesic distance transforms for gray scale images*, Pattern Recognition Letters, **17** (1996) 437-450
- [14] Trahanias P.E., Venetsanopoulos A.N., *Vector directional filters: A new class of multichannel image processing filters*, IEEE Trans. on Image Processing, **2**, 4 (1993) 528-534
- [15] Trahanias P.E., Karakos D., Venetsanopoulos A.N., *Directional processing of color images : theory and experimental results*, IEEE Trans. on Image Processing, 5, (6), 868-880, 1996

METHOD _N	NMSE [10 ⁻³]	RMSE	SNR [dB]	PSNR [dB]	NCD [10 ⁻⁴]
NONE	420.550	29.075	13.762	18.860	250.090
AMF ₁	66.452	11.558	21.775	26.873	95.347
AMF ₃	69.307	11.803	21.592	26.691	76.286
AMF ₅	91.911	13.592	20.366	25.465	75.566
VMF ₁	136.560	16.568	18.647	23.745	153.330
VMF ₃	93.440	13.705	20.295	25.393	123.500
VMF ₅	87.314	13.248	20.589	25.688	117.170
BVDF ₁	289.620	24.128	15.382	20.480	143.470
BVDF ₃	279.540	23.705	15.536	20.634	117.400
BVDF ₅	281.120	23.772	15.511	20.610	114.290
GVDF ₁	112.450	15.035	19.490	24.589	119.890
GVDF ₃	76.988	12.440	21.136	26.234	89.846
GVDF ₅	76.713	12.418	21.151	26.250	84.876
DDF ₁	150.830	17.412	18.215	23.314	143.530
DDF ₃	106.900	14.659	19.710	24.809	114.770
DDF ₅	100.500	14.213	19.979	25.077	108.960
HDF ₁	119.100	15.473	19.241	24.339	131.190
HDF ₃	72.515	12.073	21.396	26.494	99.236
HDF ₅	66.584	11.569	21.766	26.865	92.769
AHDF ₁	105.480	14.561	19.768	24.867	129.710
AHDF ₃	64.519	11.388	21.903	27.002	97.873
AHDF ₅	60.166	10.997	22.206	27.305	91.369
FVDF ₁	78.927	12.596	21.028	26.126	101.950
FVDF ₃	57.466	10.748	22.406	27.504	77.111
FVDF ₅	62.269	11.188	22.057	27.156	74.235
ANNF ₁	86.497	13.186	20.630	25.729	107.130
ANNF ₃	63.341	11.284	21.983	27.082	82.587
ANNF ₅	66.054	11.523	21.801	26.900	78.677
ANP-E ₁	66.082	11.525	21.799	26.898	95.237
ANP-E ₃	60.396	11.018	22.190	27.288	76.896
ANP-E ₅	73.416	12.148	21.342	26.441	75.456
ANP-G ₁	66.095	11.526	21.798	26.897	95.244
ANP-G ₃	60.443	11.023	22.187	27.285	76.890
ANP-G ₅	73.497	12.155	21.337	26.436	75.458
ANP-D ₁	81.306	12.784	20.899	25.997	104.980
ANP-D ₃	58.389	10.834	22.337	27.435	78.486
ANP-D ₅	63.136	11.265	21.997	27.096	75.442
SAP-2 ₁	51.869	10.211	22.851	27.950	80.682
SAP-2 ₂	45.203	9.532	23.448	28.547	69.149
SAP-2 ₃	48.918	9.916	23.105	28.204	68.676
SAP-3 ₁	50.600	10.085	22.958	28.057	74.218
SAP-3 ₂	51.396	10.164	22.891	27.989	68.796
SAP-3 ₃	58.020	10.799	22.364	27.463	70.046
SAP-Ad ₁	52.631	10.286	22.788	27.886	81.282
SAP-Ad ₂	45.018	9.513	23.466	28.565	68.579
SAP-Ad ₃	48.158	9.839	23.173	28.272	67.573
EPM ₁	60.028	10.985	22.216	27.315	79.352
EPM ₂	55.030	10.518	22.594	27.693	68.265
EPM ₃	60.099	10.991	22.211	27.310	68.914

Table 2

Comparison of the new algorithms with the standard techniques (Tab. 1) using the LENA standard image corrupted by Gaussian noise $\sigma = 30$. SAP-2, 3 denote the self avoiding path with 2 and 3 steps ($\beta = 8, \alpha = 1.2$), SAP-Ad denotes adaptive version of SAP ($\gamma = 4$, 2 steps) and EPM denotes the filter based on a model of escaping path (3 steps, $\beta = 11, \alpha = 2$). The subscripts denote the iteration number.

METHOD _N	NMSE [10 ⁻³]	RMSE	SNR [dB]	PSNR [dB]	NCD [10 ⁻⁴]
NONE	905.930	42.674	10.429	15.528	305.550
AMF ₁	128.940	16.099	18.896	23.995	122.880
AMF ₃	97.444	13.996	20.112	25.211	95.800
AMF ₅	113.760	15.122	19.440	24.539	92.312
VMF ₁	161.420	18.013	17.920	23.019	161.700
VMF ₃	104.280	14.478	19.818	24.916	128.620
VMF ₅	96.464	13.925	20.156	25.255	121.790
BVDF ₁	354.450	26.692	14.504	19.603	152.490
BVDF ₃	336.460	26.006	14.731	19.829	123.930
BVDF ₅	338.940	26.102	14.699	19.797	118.500
GVDF ₁	140.970	16.833	18.509	23.607	126.820
GVDF ₃	93.444	13.705	20.294	25.393	94.627
GVDF ₅	91.118	13.534	20.404	25.503	89.277
DDF ₁	176.670	18.845	17.528	22.627	152.050
DDF ₃	119.330	15.488	19.232	24.331	119.940
DDF ₅	110.620	14.912	19.561	24.660	113.390
HDF ₁	143.190	16.966	18.441	23.539	139.360
HDF ₃	82.413	12.871	20.840	25.939	104.620
HDF ₅	74.487	12.236	21.279	26.378	97.596
AHDF ₁	132.710	16.333	18.771	23.869	138.180
AHDF ₃	75.236	12.298	21.236	26.334	103.410
AHDF ₅	68.563	11.740	21.639	26.738	96.327
FVDF ₁	108.760	14.786	19.635	24.734	111.220
FVDF ₃	73.796	12.179	21.320	26.418	83.629
FVDF ₅	76.274	12.382	21.176	26.275	80.081
ANNF ₁	110.720	14.919	19.558	24.656	113.560
ANNF ₃	75.652	12.332	21.212	26.310	86.836
ANNF ₅	76.757	12.421	21.149	26.247	82.825
ANP-E ₁	128.590	16.077	18.908	24.007	122.890
ANP-E ₃	90.509	13.488	20.433	25.532	97.621
ANP-E ₅	96.930	13.959	20.135	25.234	94.131
ANP-G ₁	128.600	16.078	18.908	24.006	122.900
ANP-G ₃	90.523	13.489	20.432	25.531	97.603
ANP-G ₅	96.990	13.963	20.133	25.231	94.134
ANP-D ₁	113.900	15.131	19.435	24.533	115.230
ANP-D ₃	74.203	12.213	21.296	26.394	85.026
ANP-D ₅	76.265	12.381	21.177	26.275	81.202
SAP-2 ₁	65.777	11.499	21.819	26.918	87.297
SAP-2 ₂	50.597	10.085	22.959	28.057	73.008
SAP-2 ₃	51.459	10.170	22.885	27.984	71.474
SAP-3 ₁	58.580	10.851	22.322	27.421	79.256
SAP-3 ₂	54.324	10.450	22.650	27.749	71.808
SAP-3 ₃	58.441	10.839	22.333	27.431	71.510
SAP-Ad ₁	67.069	11.611	21.735	26.833	87.987
SAP-Ad ₂	51.018	10.127	22.923	28.021	72.650
SAP-Ad ₃	52.101	10.234	22.832	27.930	70.954
EPM ₁	69.468	11.817	21.582	26.681	84.310
EPM ₂	60.087	10.990	22.212	27.311	71.362
EPM ₃	65.590	11.482	21.832	26.9300	72.118

Table 3

Comparison of new algorithms with standard techniques using *LENA* image corrupted by 4% impulse and Gaussian noise $\sigma = 30$. SAP-2, 3 denote the SAP with 2 and 3 steps ($\beta = 8, \alpha = 1.2$), SAP-Ad denotes adaptive version of SAP ($\gamma = 4, 2$ steps) and EPM denotes the filter based on a model of escaping path (3 steps, $\beta = 10, \alpha = 1.4$), subscripts denote the iteration number.

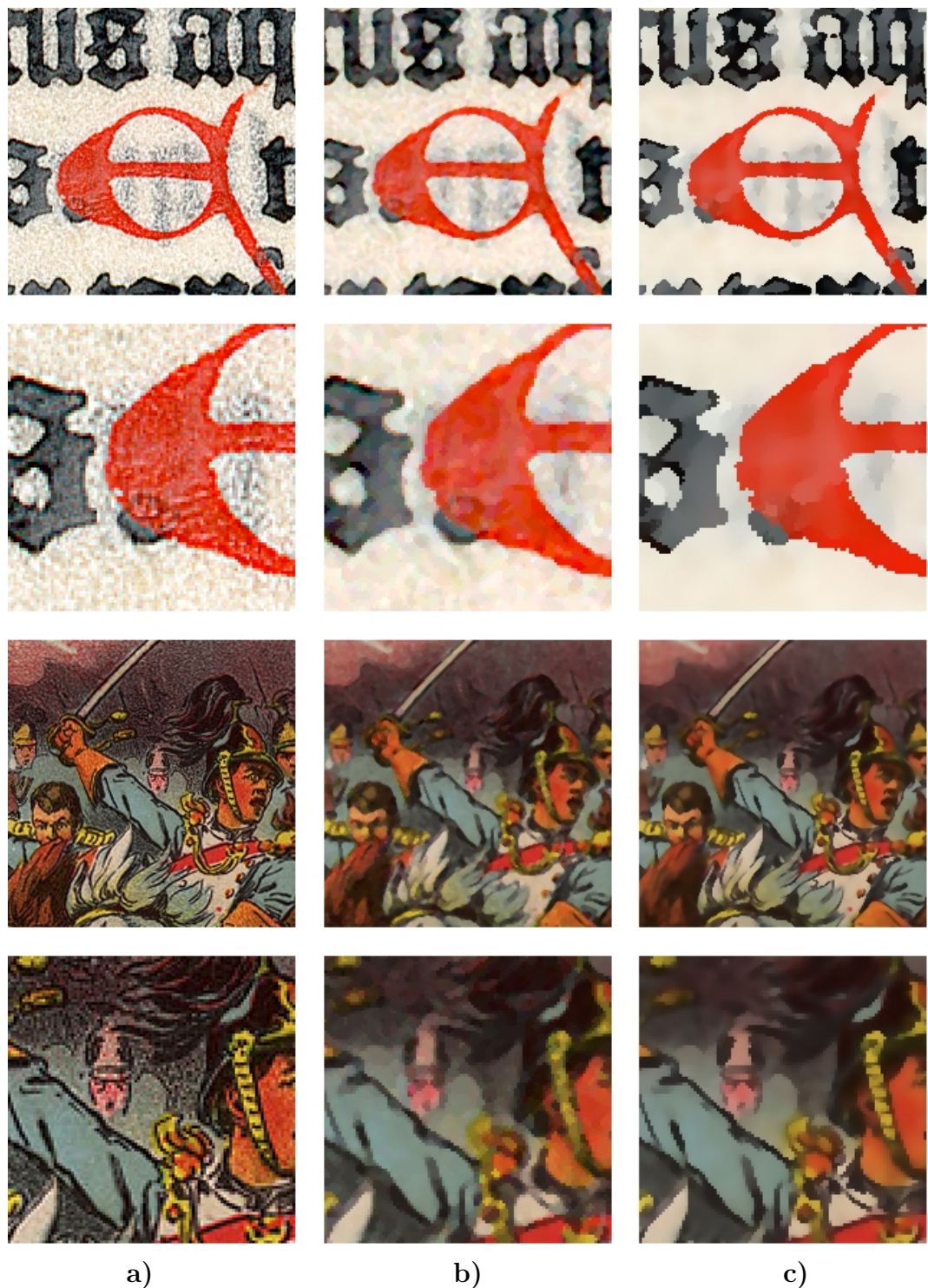


Fig. 8. Comparison of the efficiency of the vector median with the proposed noise reduction technique when Escaping Path Model is used: **a)** test images (parts of an old manuscript and a poster), **b)** result of the standard vector median filtration (3×3 mask), **c)** result of the EPM filtration ($\beta = 20, \alpha = 1.2, n = 3$, 3 iterations).



Fig. 9. Comparison of the efficiency of the vector median with the proposed noise reduction technique for *LENA* and *PEPPERS* test images. **a)** test images, **b)** result of the standard vector median filtration (3×3 mask, five iterations), **c)** result of the Adaptive SAP filtration ($\gamma = 4, n = 2$, 5 iterations).

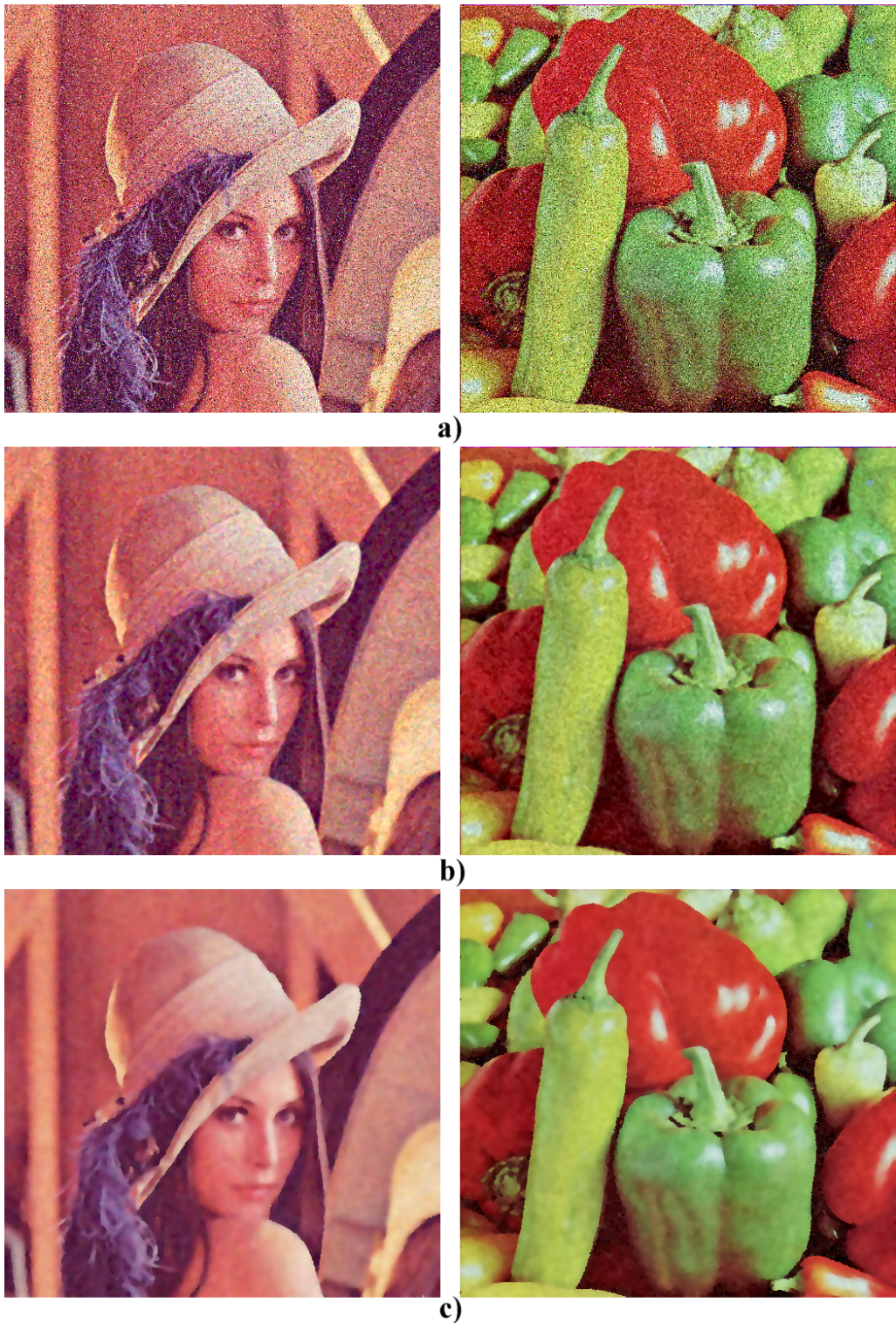


Fig. 10. Comparison of the efficiency of the vector median with the proposed noise reduction technique for *LENA* and *PEPPERS* test images: **a)** test images corrupted by 4% impulse and Gaussian noise $\sigma = 30$, **b)** result of the standard vector median filtration (3 \times 3 mask, five iterations), **c)** result of the Adaptive SAP filtration ($\gamma = 4, n = 2, 5$ iterations).